CHAPTER 14

Design of a landing strut and wing spar

The methodology for the design of a landing strut and a wing spar are discussed in this chapter. Simultaneous satisfaction of the strength and deflection are required in the design of the landing strut. The objective for the wing spar design is to determine two design variables that minimize the weight of the spar subject to constraints on material yielding, buckling, and fracture. Practice exercises in design are included for the reader to complete. The exercise in article 14.1.2 requires a re-design of the strut. The exercise in article 14.2.3 involves a monocoque spar, and the exercise in article 14.3.3 involves a stringer-stiffened spar.

14.1 Landing strut

Private aircraft are certified in the United States under the FAA Federal Aviation Regulation (FAR) Part 23 – Normal, utility, acrobatic, and commuter category. Landing gear struts, or shock struts, are designed to absorb dynamic loads due severe impact. Design of a simple steel leaf spring strut is discussed in this article, which augments the original design methodology presented by Thurston (1995). FAA design conditions require each main wheel to carry a vertical load at least equal to the airplane gross weight per FAR 23.473(g) and FAR 23 Appendix C. The gross weight of the airplane $W = 2,000$ lb., and the configuration of the landing strut is shown in figure. 14.1.

14.1.1 Strut deflection

When developing a strut design it is necessary to vary the spring strut dimensions b and h as shown in figure. 14.1 until sufficient deflection is obtained to provide acceptable vertical force load factors. If the spring strut is too stiff, the deflection is too low and the vertical load factor is high. If the spring strut is too compliant, the deflection is too large and the landing gear is springy, but the vertical load factor may be acceptable. We use Castigliano's second theorem to determine the formula for vertical deflection of the strut:

$$\Delta = \frac{\partial U^*}{\partial R}, \tag{14.1}$$

where U^* is the complementary strain energy. Energy is stored in the strut due to bending, compression, and

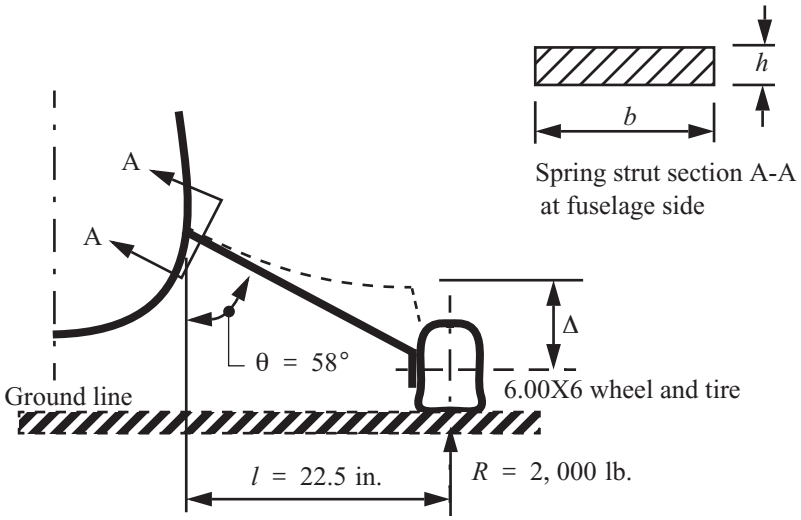

Fig. 14.1 Sketch of the steel leaf spring strut configuration.

transverse shear deformation. However, the deflection is dominated by bending, so

$$U^* = \int_0^L \left[\frac{M_x^2}{2EI_{xx}}\right] dz\,, \tag{14.2}$$

where L is the length of the strut, z is the axial coordinate; $z = 0$ @ axel, $M_x(z)$ is the bending moment, E is Young's modulus, and I_{xx} is the second area moment about the centroidal x-axis. Interchanging the derivative and definite integral in eq. (14.2), the deflection in the direction of R is

$$\Delta = \frac{\partial U^*}{\partial R} = \int_0^L \left[\frac{M_x}{EI_{xx}}\frac{\partial M_x}{\partial R}\right] dz\,. \tag{14.3}$$

To determine how the bending moment, axial force, and shear force depend on R, impose static equilibrium conditions on the strut. From the free-body diagram shown in figure. 14.2, we get

$$V_y + R\sin\theta = 0 \qquad N + R\cos\theta = 0 \qquad M_x + zR\sin\theta = 0 \qquad 0 \le z \le L\,. \tag{14.4}$$

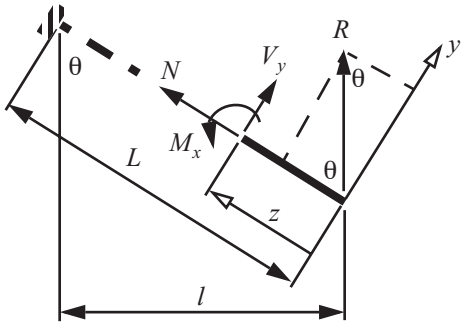

Fig. 14.2 Free body diagram of the strut.

Substitute the bending moment from eq. (14.4) into eq. (14.3) to find

$$\Delta = \frac{1}{EI_{xx}}\int_0^L (-zR\sin\theta)(-z\sin\theta)dz = \frac{RL^3\sin^2\theta}{3EI_{xx}}. \tag{14.5}$$

The horizontal length $l = L\sin\theta$. Eliminate strut length in terms of the horizontal length in eq. (14.5) to get

$$\Delta = \frac{Rl^3}{3EI_{xx}\sin\theta}. \tag{14.6}$$

Take the strut to be made of steel having a Young's modulus of 30×10^6 psi. Consider an initial size of

$$b = 3.0 \text{ in.} \qquad h = 0.69 \text{ in.} \tag{14.7}$$

The cross-sectional area $A = 3(0.69) = 2.07$ in.^{2} .The second area moment about the centroidal x-axis in the cross section is

$$I_{xx} = \frac{bh^3}{12} = \frac{3(0.69)^3}{12} = 0.0821 \text{ in.}^4 \tag{14.8}$$

Numerical evaluation of the strut deflection is

$$\Delta = \frac{(2,200 \text{ lb.})(22.5 \text{ in.})^3}{3(30 \times 10^6 \text{ lb./in.}^2)(0.0821 \text{ in.}^2)\sin 58°} = 4.00 \text{ in.} \tag{14.9}$$

The stopping distance d is equal to the stroke of the strut plus the tire deflection. From 6.00X6 tire deflection charts at an inflation pressure of 20 psi, the tire deflection is 3.14 in. at 2,200 lb. loading. Hence,

$$d = \Delta + 3.14 \text{ in.} = 7.14 \text{ in.} = 0.595 \text{ ft.}. \tag{14.10}$$

According to FAR 23.473(d), the initial descent velocity, in feet per second, for landing gear design calculations cannot be less than $4.4(W/S)^{1/4}$, where W is the gross weight in pounds and S is the wing reference area in sq. ft. Assuming $S = 157$ ft.^{2} we get $V_d = 8.5$ ft./s. Now assume the acceleration of the mass center is constant during the period of landing. Let descent velocity at touchdown be denoted by V_d, and during the period of landing the vertical speed reduces from V_d to zero. The acceleration of the mass center is computed from the uniform acceleration formula given by eq. (2.14) on page 12. See figure. 14.3.

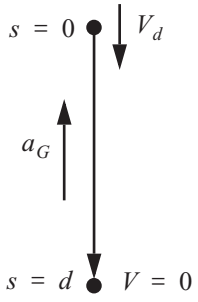

Fig. 14.3 Uniform deceleration along a straight line.

$$a_G = V_d^2/(2d) = \frac{(8.5)^2}{2(0.595)} = 60.714 \text{ ft/s}^2. \tag{14.11}$$

The load factor at touchdown is

$$n = 1 + \frac{60.714}{32.2} = 2.89. \tag{14.12}$$

The load reduction due to wing lift is 0.67 as stipulated in FAR 23.473(e), so the landing gear limit load factor is

$$n = 2.89 - 0.67 = 2.2. \tag{14.13}$$

Strength consideration. The axial normal stress is due to the superposition of the bending component and the compression component.

$$\sigma_z = \frac{M_x y}{I_{xx}} + \frac{N}{A} \qquad -\frac{h}{2} \le y \le \frac{h}{2} \qquad 0 \le z \le L\,. \tag{14.14}$$

Substitute M_x and N from eq. (14.4), and substitute I_{xx} from eq. (14.8), into eq. (14.14) to get

$$\sigma_z = \frac{-zR\sin\theta(h/2)}{(bh^3)/12} - \frac{R\cos\theta}{bh} = \frac{-6zR\sin\theta}{bh^2} - \frac{R\cos\theta}{bh}\,. \tag{14.15}$$

The axial normal stress (14.15) attains maximum magnitude at $z = L$. For $b = 3$ in. and $h = 0.69$ in. the maximum magnitude is

$$\sigma_z\big|_{z=L} = -208,503. - 563.2 = -209,066.2 \text{ psi}\,.$$

Steel alloy 4340, oil quenched and tempered, has a yield strength of 230 ksi and an ultimate tensile strength of 250 ksi. A major application of alloy 4340 is to aircraft landing gears because of its high strength. For design assume an allowable stress of 160 ksi, which implies a factor of safety of 1.4 with respect to yield. The margin of safety is defined by

$$MS = \frac{\text{excess strength}}{\text{required strength}} = \frac{\sigma_{\text{alllowable}} - |\sigma_z|_{\max}}{|\sigma_z|_{\max}}\,. \tag{14.16}$$

The margin of safety is positive for a feasible design, and negative for an infeasible design. For the design $b = 3$ in. and $h = 0.69$ in., the $MS = -0.233$. Therefore, with respect to strength the design (14.7) is infeasible.

Moreover, the landing gear limit load factor is specified as 2.0 in FAR 23.473(g), and not the 2.2 determined for the initial design (14.7). To achieve the required landing gear load factor we compute new values for the acceleration, the stopping distance and the stroke of the strut as follows:

$$a_G = (2 - 1 + 0.67)g = 53.77 \text{ ft./s}^2 \qquad d = V_d^2/(2a_G) = 8.09 \text{ in.} \qquad \Delta = d - 3.14 = 4.95 \text{ in.}\,. \tag{14.17}$$

The new second area moment for the leaf spring strut is obtained by a rearrangement of (14.9):

$$I_{xx} = \frac{Rl^3}{3E(4.95)\sin\theta} = 0.06638 \text{ in.}^4 = \frac{bh^3}{12}\,. \tag{14.18}$$

Solve eq. (14.18) for h to get

$$h = 0.9269883/b^{1/3}\,. \tag{14.19}$$

Substitute eq. (14.19) for h into axial normal stress (14.15) and evaluate it at $z = L$ to get

$$\sigma_z = \frac{-1,257.65}{b^{2/3}} - \frac{345,632.}{b^{1/3}}\,. \tag{14.20}$$

Set $|\sigma_z| = 160,000$ psi in eq. (14.20), and by a root finding routine, or by a trial and error method, find

$$b = 10.13 \text{ in.} \qquad h = 0.4284 \text{ in.} \tag{14.21}$$

For the design (14.21), the margin of safety (14.16) is positive for $0 \le z \le L$ as shown in figure. 14.4. At $z = L = 26.53$ in. it is $6.7\times10^{-16} \sim 0$ and at $z = 0$ it is 594.7. The design (14.21) is feasible with respect to strength and also satisfies the landing gear load factor of 2.

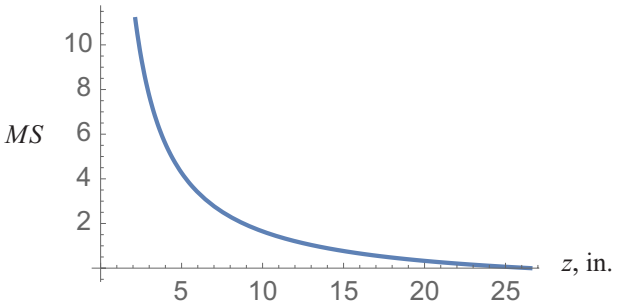

Fig. 14.4 Distribution of the margin of safety along the length of the strut for design (14.21).

14.1.2 Strut design exercise

Although the margin of safety is positive along the length of the strut in figure. 14.4, it is very large over most of the length of the strut. An efficient use of material to carry the load has a margin of safety that is sightly positive. The large positive values of the margin of safety shown in figure. 14.4 indicate that the design is too heavy. The specific weight of steel is 0.284 lb./in.^{3}, so the weight of the leaf spring strut (14.21) is

$$W = (0.284 \text{ lb./in.}^3)(10.13 \text{ in.})(0.4284 \text{ in.})(26.53 \text{ in.}) = 32.7 \text{ lb.} \tag{14.22}$$

Since the axial normal stress (14.15) is linear in the coordinate z, it is reasonable to assume that the cross-sectional area of the strut should be linear in z. Take the thickness of the strut h to be independent of z, and let the width of the strut be a linear function of z. That is,

$$b(z) = b_L\left(\frac{z}{L}\right) + b_0\left(1 - \frac{z}{L}\right) \qquad 0 \le z \le L\,, \tag{14.23}$$

where b_0 is the width at the axel and b_L is the width at the fuselage. Of course, this means that the second area moment of the cross section, $I_{xx} = (bh^3)/12$, is a linear function of z.

1. Determine the value of the design variables h, b_0, and b_L such that stroke is equal to 4.95 in. and the magnitude of the normal stress σ_z is less than, or equal to, an allowable value of 160,000 psi.

2. Plot the margin of safety for strength of the design in step 1 with respect to z for $0 \le z \le L$.

3. Compute the weight of the design determined in step 1.

14.2 Wing spar design

The wing spar is the primary load bearing structure in the wing. Consider the design of a spar for minimum weight under a particular maneuver condition subject to different design limit states. The example is the Mohawk commuter airplane shown in figure. 14.5. The wing is slightly tapered, but to simplify the analysis we will treat it as uniform. The wing span is 74 feet, and the wing area is 592 square feet, so that the average chord is 8 feet. About 9 feet of this wing span is the fuselage width, so that we will assume that each wing is a 32.5-foot-long cantilever beam. At the root of the wing, the airfoil is NACA 23016, with a thickness-to-chord ratio (t/c) of 16

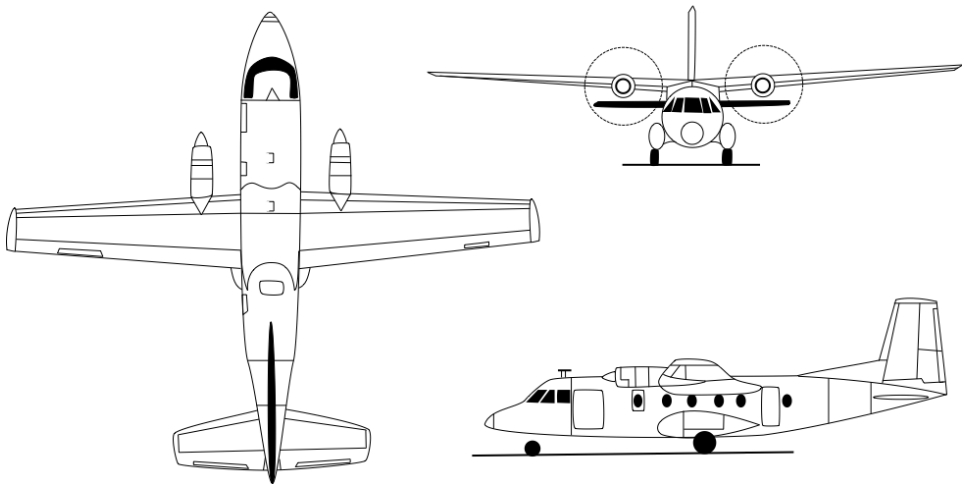

Fig. 14.5 Mohawk 298 commuter airplane

percent, while at the tip, the airfoil is NACA 32012, with a thickness-to-chord ratio of 12 percent. Assume a constant $t/c = 0.14$, corresponding to a maximum thickness of the airfoil of 1.12 ft.

Design load condition. The load condition that usually designs most of the wing box is a pull-up maneuver. For transport aircraft the FAA specifies a maneuver of 2.5 g, with a safety factor of 1.5. That is, the wings need to be able to carry about 2.5 times the weight of the airplane without suffering material failure. The maximum takeoff weight is 23,810 lb., but in this condition there is a lot of fuel in the wing, and this fuel provides inertia relief, reducing the stresses in the wing. Also, part of the lift of the wing is provided by the area over the fuselage, so we will assume that the two wings carry 20,000 lb. in cruise, and 50,000 lb. in the design pull-up maneuver.

Wing box overall dimensions. Assume a wing box that is 24 in. in the chord-wise direction and 13 in. deep so that it can fit into the airfoil. See figure. 14.6.

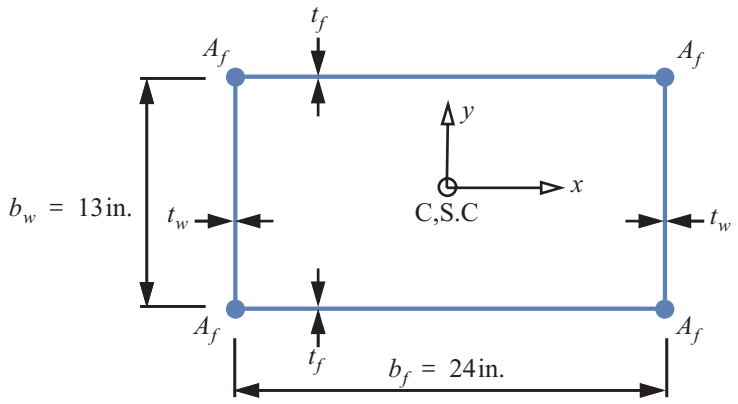

Fig. 14.6 Semimonocoque wing spar cross section. Design variables are the thicknesses t_f and t_w, and the stringer flange area A_f.

Material data. 1.The wing is made of aluminum alloy 2024-T351 with Young's modulus of

$E = 10\times10^6$ psi, Poisson's ratio of 0.3, a specific weight of 0.1 lb./in.^{3}, a yield strength in tension or compression of 47,000 psi, and a mode I fracture toughness $K_{Ic} = 31,000 \text{ psi}\sqrt{\text{in.}}$

Spanwise airload distribution. Let z denote the spanwise axis along the locus of shear centers of each cross section. The z-axis measured from the root to tip, with $0 \le z \le z_{max}$, and $z_{max} = 32.5 \times 12 = 390$ in. Assume that the load is distributed elliptically over the wing as in example 6.6 on page 165, so that the load intensity f_L per unit span is given as

$$f_L(\zeta) = \frac{2L}{\pi z_{max}}\sqrt{1-\zeta^2} \qquad 0 \le \zeta \le 1 \qquad \zeta = \frac{z}{z_{max}}, \tag{14.24}$$

where the total lift $L = 50,000$ lb., and the wing span $z_{max} = 32.5$ ft.

It is given that the line of action of the lift is acting on the front web of the box beam. Equilibrium conditions shown in figure. 14.7 determine the shear force, bending moment, and torque at the wing root as

$$V_y(0) = \frac{L}{2} = 25,000 \text{ lb.} \qquad M_x(0) = \frac{-2Lz_{max}}{3\pi} = -4.13803\times10^6 \text{ lb.-in.} \qquad M_z(0) = \left(-\frac{b_f}{2}\right)\frac{L}{2} = -300,000 \text{ lb.-in.}$$

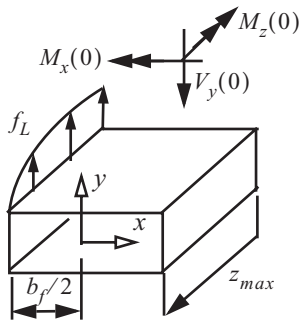

$$-V_y(0) + z_{max}\int_0^1 f_L(\zeta)d\zeta = 0$$

$$-M_x(0) - z_{max}^2\int_0^1 \zeta f_L(\zeta)d\zeta = 0$$

$$-M_z(0) - \left(\frac{b_f}{2}\right)z_{max}\int_0^1 f_L(\zeta)d\zeta = 0$$

Fig. 14.7 Free body diagram of the spar and the equilibrium equations.

14.2.1 Evaluation of stresses at root cross section

Since the wing box is uniform along the span, the thicknesses are sized by the conditions at the root. Ten locations for evaluation of the Mises effective stresses and the margins of safety are shown in figure. 14.8.

The axial normal stress at the root due to flexure is determined from eq. (4.6) on page 79. For this symmetric cross section we get from eq. (4.4) that $n_x = n_y = 0$, $k = 1$., and $\bar{y}(s) = y(s)$ by eq. (4.7). In the absence of an axial normal force and no thermal loads, the normal stress in eq. (4.6) reduces to

$$\sigma_{zz} = \frac{M_x(0)}{I_{xx}}y(s). \tag{14.25}$$

The second area moment about the x-axis through the centroid of the cross section is given by

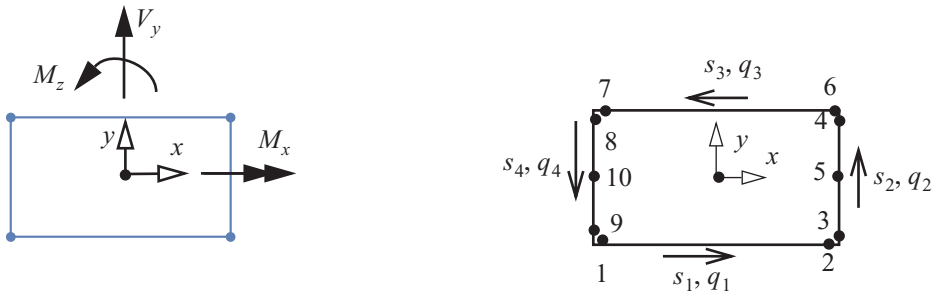

Resultants **Mises stress locations**

Fig. 14.8 Locations for the evaluation of stresses at the wing root.

$$I_{xx} = A_f b_w^2 + (b_f b_w^2 t_f)/2 + (b_w^3 t_w)/6 . \tag{14.26}$$

The shear stresses tangent to the contour are determined from the shear flows and thicknesses of the panels of the box beam (i.e., $\sigma_{zs} = q(s,z)/t(s)$). For the box beam the shear stresses in each branch are

$$\sigma_{zs}\big|_i = \tau_i(s_i) = q_i(s_i)/t_i \qquad i = 1, 2, 3, 4 , \tag{14.27}$$

where $q_i(s_i)$ denotes the shear flow in the *i-th* branch, and s_i denotes the branch contour coordinate. The total shear flows are the summation of the shear flow due to the transverse shear force acting through the shear center and the torque. From eq. (4.25) on page 82, the total shear flow at a given contour location is

$$q_i(s_i) = \frac{M_z(0)}{2A_c} - F_y(s_i)V_y(0) \qquad i = 1, 2, 3, 4 . \tag{14.28}$$

The shear flow distribution function with respect to the shear center $F_y(s)$ is obtained from eq. (4.19) and eq. (4.26), where $x_{sc} = 0$. For each branch we write

$$F_y(s_i) = \frac{1}{I_{xx}}\left[Q_{xi}(s_i) - \frac{1}{2A_c}\left[\oint r_n Q_x ds\right]\right], \tag{14.29}$$

where the area enclosed by the cell $A_c = b_f b_w$. The functions $Q_{xi}(s_i)$ in eq. (14.29) are distribution functions defined by first area moments, and are obtained from eq. (4.9) on page 80. For each branch functions $Q_{xi}(s_i)$ are determined from

$$Q_{x1}(s_1) = \left(\frac{-b_w}{2}\right)A_f + \int_0^{s_1} y_1(s_1)t_f ds_1 , \; Q_{x2}(s_2) = Q_{x1}(b_f) + \left(\frac{-b_w}{2}\right)A_f + \int_0^{s_2} y_2(s_2)t_w ds_2 ,$$

$$Q_{x3}(s_3) = Q_{x2}(b_w) + \left(\frac{b_w}{2}\right)A_f + \int_0^{s_3} y_3(s_3)t_f ds_3 , \text{ and } Q_{x4}(s_4) = Q_{x3}(b_f) + \left(\frac{b_w}{2}\right)A_f + \int_0^{s_4} y_4(s_4)t_w ds_4 . \tag{14.30}$$

The contour coordinate functions $[x(s), y(s)]$, functions $Q_{xi}(s_i)$, and the evaluation of coordinates normal to

contour r_{ni} are listed in table 14.1.

Table 14.1 Geometric functions of the contour

Branch	s_i	x_i	y_i	Qx_i	$r_{ni,}$ eq. (4.11)
i =1	$0 \le s_1 \le b_f$	$-(b_f)/2 + s_1$	$-b_w/2$	$(-b_w t_f s_1)/2$	$b_w/2$
i = 2	$0 \le s_2 \le b_w$	$b_f/2$	$(-b_w)/2 + s_2$	$-\frac{b_f b_w t_f}{2} - \frac{b_w t_w s_2}{2} + \frac{t_w s_2^2}{2}$	$b_f/2$
i = 3	$0 \le s_3 \le b_f$	$b_f/2 - s_3$	$b_w/2$	$-\frac{b_f b_w t_f}{2} + \frac{b_w t_f s_3}{2}$	$b_w/2$
i = 4	$0 \le s_4 \le b_w$	$(-b_f)/2$	$b_w/2 - s_4$	$\frac{b_w t_w s_4}{2} - \frac{t_w s_4^2}{2}$	$b_f/2$

From the results listed in table 14.1, the integral term on the right-hand side of eq. (14.29) evaluates as

$$\frac{1}{2A_c}\oint [r_n Q_x]ds = -\left(A_f b_f b_w^2 + \frac{b_f^2 b_w^2 t_f}{2}\right)/2b_f b_w . \tag{14.31}$$

The shear flow distribution functions are given in eq. (14.32) below.

$$\begin{aligned} F_y(s_1) &= \frac{b_w t_f (b_f - 2s_1)}{4I_{xx}} & F_y(s_2) &= -\left(\frac{2A_f b_w + b_f b_w t_f + 2(b_w - s_2)s_2 t_w}{4I_{xx}}\right) \\ F_y(s_3) &= \frac{-b_w t_f (b_f - 2s_3)}{4I_{xx}} & F_y(s_4) &= \frac{2A_f b_w + b_f b_w t_f + 2(b_w - s_4)s_4 t_w}{4I_{xx}} \end{aligned} . \tag{14.32}$$

Strength limit state. The Von Mises criterion given by eq. (4.31) on page 84 is used to predict the initiation of material yielding. The Mises effective stress is defined by

$$\sigma_{\text{Mises}} = \sqrt{\sigma_{zz}^2 + 3\sigma_{zs}^2} . \tag{14.33}$$

If $\sigma_{\text{Mises}} < \sigma_{\text{yield}}$, then the material response is elastic, and if $\sigma_{\text{Mises}} = \sigma_{\text{yield}}$ yielding initiates. The margin of safety (14.16) in this case is

$$MS = \frac{\sigma_{\text{allowable}} - \sigma_{\text{Mises}}}{\sigma_{\text{Mises}}} = \frac{\sigma_{\text{allowable}}}{\sigma_{\text{Mises}}} - 1 . \tag{14.34}$$

The allowable stress for the strength limit state is the yield strength of the material divided by the factor of safety (FS). That is

$$\sigma_{\text{allowable}} = \sigma_{\text{yield}}/(FS) . \tag{14.35}$$

The margin of safety is nonnegative for a feasible design, otherwise the design is infeasible. It should be zero or a small positive number.

14.2.2 Trial design of the monocoque box beam spar

A computer program was written to evaluate the Mises effective stresses at the ten locations of the root cross section using a factor of safety of 1.5. For $t_f = 0.40$ in., $t_w = 0.30$ in., and $A_f = 0$ the weight of the spar is 1, 053. lb. The values of the ten margins of safety for this design are listed in table 14.2.

Table 14.2 Margins of safety for the trial design

MS_1	0.0528	MS_6	0.0714
MS_2	0.0714	MS_7	0.0528
MS_3	0.0702	MS_8	0.0378
MS_4	0.0702	MS_9	0.0378
MS_5	9.086	MS_{10}	2.619

Since the margins of safety are all positive, this design is feasible. Although feasible, this design is too heavy and, consequently, not optimal. Lower weight feasible designs will have a nonnegative minimum margin of safety close to zero.

To aid in the search for the best design, consider the design plane shown in figure. 14.9. The thickness t_f is the abscissa and the thickness t_w is the ordinate. Each point in the plane represents a design, some are feasible some are not. Contours of constant margins of safety and constant spar weights are plotted in the design plane[1]. Only designs with a nonnegative margin of safety are feasible. The least weight design occurs at a point (t_f^*, t_w^*) on the margin of safety contour equal to zero. A second condition is needed to determine point (t_f^*, t_w^*). This second condition is to equate the slope $t_w/t_f = -\left(\frac{\partial MS}{\partial t_f}\right) / \frac{\partial MS}{\partial t_w}$ on the margin of safety contour $MS = 0$ to the slope of the constant weight contour $t_w/t_f = (-b_f)/b_w$. That is, the point (t_f^*, t_w^*) on the contour $MS = 0$ is tangent to the contour of least weight.

14.2.3 Design exercise A

Write a computer program to find the thicknesses t_f and t_w of the wing box for $A_f = 0$ that will minimize the weight and carry the load without experiencing material yield using a factor of safety of 1.5. Calculate the weight of the spar and the margins of safety at the ten locations shown in figure. 14.8. Although the design given in article 14.2.2 is too heavy, it can be used to assess if the computer program is correct. Include a print out of the program and the output for the best design, which includes the ten margins of safety and the weight.

1. Fig. 14.9 was generated by the *Mathematica* function **ContourPlot[Min[MS[tf,tw,0]] == 0, {tf, 0.3, 0.8},{tw, 0.0, 0.3}]**, where definition of function **MS[tf,tw,Af]** is determined by eq. (14.34) and the ten points shown in figure. 14.8.

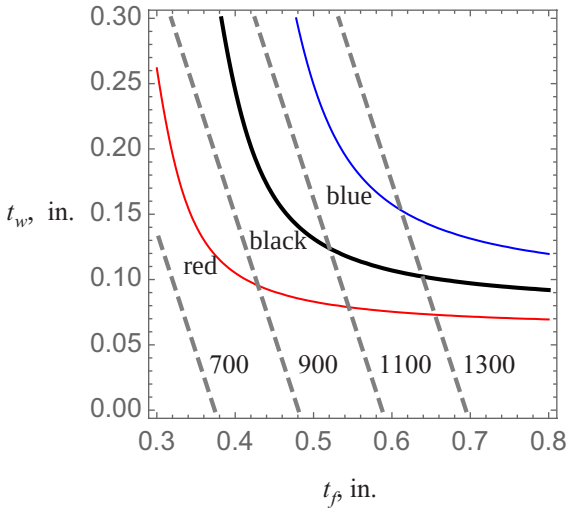

red contour: $MS = -0.2$

black contour: $MS = 0$

blue contour: $MS = 0.2$

dashed contour: spar weights in lb.

Fig. 14.9 Design plane for $A_f = 0$. Contours of the margin of safety for yield and contours of constant spar weights.

14.3 Additional limit states for buckling and fracture

Consider design variables $t_f > 0$, $t_w > 0$, and $A_f \geq 0$ for the Mohawk 298 wing spar subject to constraints on yielding, buckling, and fracture. The locations in the cross section at the wing root where the design constraints are evaluated are shown in figure. 14.10.

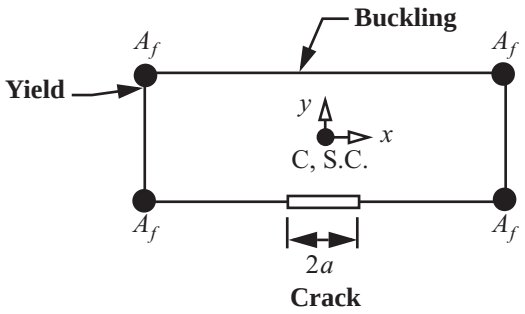

Fig. 14.10 Cross section of the stringer-stiffened box beam, and locations of constraint evaluations

14.3.1 Buckling margin of safety

Let rib spacing along the span, or z-axis, at the root of the wing be denoted by a_r, and take $a_r = b_f/2$. The upper cover skin, or branch 3 with coordinates $[x_3(s_3), y_3]$, is subject to compression and shear. The normal stress is $\sigma_{zz} = (M_x y_3)/I_{xx}$ and the shear stress $\tau_3(s_3)$ is a linear function in the contour coordinate s_3. Assume the skin can be modeled as simply supported flat plate between stiffeners for the buckling analysis. From eq. (11.118) on page 355 the combined compression and shear index for buckling is defined by

$$f_b = \left(\frac{\tau_{\text{ave}}}{\tau_{\text{cr}}}\right)^2 + \left(\frac{|\sigma_z|}{\sigma_{\text{cr}}}\right), \tag{14.36}$$

where $0 \le f_b < 1$ for no buckling and $f_b = 1$ at the onset of buckling. The average shear stress is

$$\tau_{\text{ave}} = \left(\frac{1}{b_f}\right)\int_0^{b_f} \tau_3(s_3)\,ds_3\,. \tag{14.37}$$

The critical stresses for compression (11.110) and shear (11.116) are

$$\sigma_{cr} = k_c \frac{\pi^2 E}{12(1-\nu^2)}\left(\frac{t_f}{b_f}\right)^2 \qquad \tau_{\text{cr}} = k_s \frac{\pi^2 E}{12(1-\nu^2)}\left(\frac{t_f}{b_f}\right)^2. \tag{14.38}$$

The buckling coefficients are

$$k_c = \left(\frac{1}{(a_r/b_f)} + \left(\frac{a_r}{b_f}\right)\right)^2 = 6.25 \qquad k_s = 4.22565 + \frac{5.19931}{a_r/b_f} = 14.624\,. \tag{14.39}$$

The margin of for the buckling limit state is

$$MS_b = \frac{1-f_b}{f_b}\,. \tag{14.40}$$

14.3.2 Fracture margin of safety

The design damage condition is a through crack centered in the lower left skin that is 1.00 in. long ($2a = 1.00$ in.) with the crack faces perpendicular to the *z*-axis. The lower skin, or branch 1 with coordinates $[x_1(s_1), y_1]$, is subject to a tensile stress $\sigma_{zz} = (M_x y_1)/I_{xx}$ and a shear stress $\tau_1(s_1)$ that is a linear function of contour coordinate s_1. Thus, the crack is exposed to tension and shear, which leads to mixed mode cracking (i.e., a mixture of mode I and mode II). The stress intensity factor for mode I is $K_I = \sigma_{zz}\sqrt{\pi a}$, and the stress intensity factor for mode II is $K_{II} = \tau_1\sqrt{\pi a}$. The fracture toughness for mode I loading only is K_{Ic}, and the fracture toughness for mode II loading only is K_{IIc}. A fracture criterion for mixed mode loading is given by eq. (13.42) on page 391. The plane strain fracture toughness for mode I loading is usually readily available in the literature, but the mode II fracture toughness is not usually available. Tests for mode II are more difficult to design than for mode I. Usually mode II loading does not lead to fracture (Anderson, 1995)[1]. In other words $K_{IIc} > K_{Ic}$. In addition for the design $(t_f, t_w, A_f) = (0.4, 0.3, 0)$, the stresses at the center of branch 1 are $\sigma_{zz} = 29,202.8$ psi and $\tau_3(b_f/2) = -1,201.92$ psi. The shear stress is about 4 percent of the normal stress, and so it is expected that shear would have a small influence on fracture. Thus, we assume fracture is in mode I. The margin of safety for fracture is

$$MS_f = \frac{K_{Ic}/(FS_f) - K_I}{K_I}, \tag{14.41}$$

1. Mode II loading is important if there is weak interface in the material, which is the case for delamination of filamentary composites as discussed in article 13.7 on page 392.

where the factor of safety for fracture is specified as $FS_f = 1.2$.

14.3.3 Design exercise B

Consider a longitudinally stiffened configuration of the wing box for the Mohawk 298 commuter airplane described in article 14.3. Write a computer program to determine the thicknesses t_f and t_w of the wing box for selected values of the flange area A_f listed in the table below. The objective is to minimize the weight. The design limit states are material yield (14.34) using a factor of safety of 1.5, that the compression panel of the upper skin does not buckle (14.40), and that the crack in the lower panel does not propagate (14.41). Evaluate the margin of safety for yield at point 8 shown in figure. 14.8. The minimum margin of safety should not be negative for a feasible design, but should be a small positive number. Write a computer program to determine the thicknesses t_f and t_w of the wing box for selected values of the flange area A_f listed in table 14.3.

Table 14.3 Design exercise B

A_f, in.^{2}	t_f, in.	t_w, in.	weight, lb.	Margins of safety		
				Yield	Buckling	Fracture
0						
1.0						
2.0						
3.0						

14.4 References

Anderson, T.L. ***Fracture Mechanics***, 2d ed. Boca Raton, FL: CRC Press Inc., 1995, p. 87.

Dowling, N. ***Mechanical Behavior of Materials***. Englewood Cliffs, NJ: Prentice-Hall, Inc., 1993, pp. 245-252.

Thurston, David B. ***Design For Flying***. 2d ed. New York: TAB Books, a Division of McGraw-Hill, Inc., 1995, pp. 237-245.